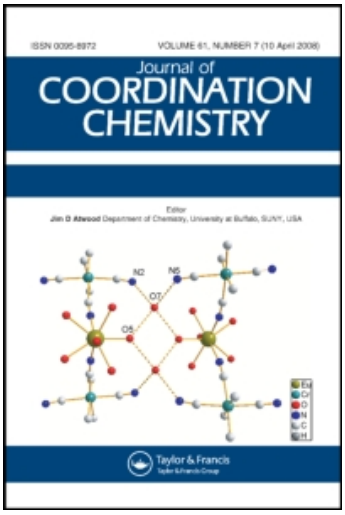

Journal of Coordination Chemistry
Publication details, including instructions for authors and subscription information:
http://www.informaworld.com/smpp/title~content=t713455674

Triclinic structural isomer of cerium(III)-picrate complexes with triethylene glycol

Eny Kusrini[a]; Muhammad I. Saleh[b]; Rohana Adnan[b]; Hoong-Kun Fun[c]; Bohari M. Yamin[d]
[a] Faculty of Engineering, Department of Chemical Engineering, University of Indonesia, 16424 Depok, Indonesia [b] School of Chemical Sciences, Universiti Sains Malaysia, 11800 Penang, Malaysia [c] School of Physics, University Sains Malaysia, 11800 Minden, Penang, Malaysia [d] School of Chemical Sciences and Food Technology, Universiti Kebangsaan Malaysia, 43600 Bangi, Selangor, Malaysia

First published on: 18 January 2010

To cite this Article Kusrini, Eny , Saleh, Muhammad I. , Adnan, Rohana , Fun, Hoong-Kun and Yamin, Bohari M.(2010) 'Triclinic structural isomer of cerium(III)-picrate complexes with triethylene glycol', Journal of Coordination Chemistry, 63: 3, 484 — 497, First published on: 18 January 2010 (iFirst)
To link to this Article: DOI: 10.1080/00958970903515142
URL: http://dx.doi.org/10.1080/00958970903515142

Journal of Coordination Chemistry
Vol. 63, No. 3, 10 February 2010, 484–497

Taylor & Francis
Taylor & Francis Group

Triclinic structural isomer of cerium(III)–picrate complexes with triethylene glycol

ENY KUSRINI*†, MUHAMMAD I. SALEH*‡, ROHANA ADNAN‡, HOONG-KUN FUN§ and BOHARI M. YAMIN¶

†Faculty of Engineering, Department of Chemical Engineering, University of Indonesia, 16424 Depok, Indonesia
‡School of Chemical Sciences, Universiti Sains Malaysia, 11800 Penang, Malaysia
§School of Physics, University Sains Malaysia, 11800 Minden, Penang, Malaysia
¶School of Chemical Sciences and Food Technology, Universiti Kebangsaan Malaysia, 43600 Bangi, Selangor, Malaysia

(*Received 24 June 2008; in final form 9 September 2009*)

Two new isomers of $[Ce(NO_3)(Pic)(H_2O)_2(EO3)](Pic)$ complex (where EO3 = triethylene glycol and Pic = picrate anion) have been synthesized by one-pot reaction and structurally characterized. Both isomers, orange and yellow in color, respectively, have a triclinic *P-1* crystal lattice with different unit cell dimension, and Ce(III) adopts a different coordination number. In orange isomer, the Pic anion is chelated to Ce(III) via phenolic and *ortho*-nitro oxygens in a bidentate mode, while in yellow isomer the Pic anion is chelated only monodentate through the phenolic oxygen. Coordination geometries can be described as a distorted bicapped square antiprism and a distorted tricapped trigonal prism for **1** and **2**, respectively. Alcohol groups from EO3 form a 1-D chain with symmetry direction [1 0 0] through intermolecular O–H···O hydrogen bonding. Photoluminescence spectra of the complexes showed a broad band at 515–540 nm due to the 5d → 4f transition from the Ce(III) with electric dipole allowed.

Keywords: Cerium; Picrate complexes; Triethylene glycol

1. Introduction

Coordination and structural chemistry of Ln(III) complexes with oxygen donors from polyether ligands has attracted interest due to their unique structural characteristics, ability to adopt different geometries and structural diversity [1–3]. The physical and chemical properties of the host–guest complexes are determined not only by the nature of the $Ln–O_{ligand}$ coordination bonds but also by the geometric arrangement of the ligands around the Ln(III) ion.

Ln–EO3 complexes form salt-type compounds with a general molecular formula of $[Ln(H_2O)_mX_a(EO3)_n]X_b$ with EO3 = triethylene glycol, $n = 1–3$, $m = 1–6$, $a = 1–2$,

*Corresponding authors. Email: ekusrini@che.ui.ac.id; midiris@usm.my

Journal of Coordination Chemistry
ISSN 0095-8972 print/ISSN 1029-0389 online © 2010 Taylor & Francis
DOI: 10.1080/00958970903515142

$b = 1$–3, X = halogen, NO_3^-, ClO_4^-, or SCN^- depending on the Ln(III) ion and the anion. Structures of the series of the lanthanide complexes with different polyethylene glycol (PEG) chain lengths and counteranion, i.e., Cl^-, SCN^-, and NO_3^- have been reported by Rogers *et al*. [1]. Coordination number of the lanthanide complexes with the EO3 ligand are between 9 and 11 as shown by $[La(NCS)_3(H_2O)_2(EO3)] \cdot 0.5H_2O$ [1], $[Nd(NO_3)_3(EO3)]$ [4], $[CeCl(H_2O)(EO3)_2]Cl_2$ [5], $[CeCl_2(H_2O)_2(EO3)]_2Cl_2$ [5], and $[Ce(NO_3)_3(H_2O)(EO3)] \cdot CH_3CN$ [6].

In previous study, we observed the consistency of monoclinic polymorph of lanthanide with the EO3 ligand in the presence of picrate anion (Pic), namely $[La(Pic)_2(EO3)_2](Pic)$ complexes, when we synthesized the lanthanum-picrate with the EO3 ligand by two different preparations [7]. We assumed that changes in conformation, arrangement, atom connectivity in the crystal packing of Ln–Pic–EO3 can occur without any changes in their composition, even though we change the central lanthanide ion. To evaluate this assumption, we have systematically studied Ln–EO3–Pic complex with the Ce(III). In this article, we report the synthesis, characterization, crystal structures, and photoluminescence (PL) properties of $[Ce(NO_3)(Pic)(H_2O)_2(EO3)](Pic)$.

2. Experimental

2.1. *Chemicals and materials*

EO3 [$C_6H_{14}O_4$] (99% purity) and $Ce(NO_3)_3 \cdot 6H_2O$ (99.9% purity) were purchased from Acros (New Jersey, USA) and Johnson Matthey Electronics (New Jersey, USA), respectively. Picric acid (HPic), [$(NO_2)_3C_6H_2OH$, >98% purity) was purchased from BDH (Poole, UK). Other chemicals are of analytical grade and used without purification.

2.2. *Synthesis of the Ce–Pic–EO3 complex*

The complex was prepared as previously described [7]. A mixture of EO3 (0.454 g, 3.0 mmol), HPic (0.917 g, 4 mmol), and $Ce(NO_3)_3 \cdot 6H_2O$ (0.434 g, 1 mmol) was dissolved in 30 mL acetonitrile : methanol : water (3 : 3 : 1 v/v). This mixture was stirred for 10 min at room temperature. The beaker was covered loosely with aluminum foil to allow slow evaporation at room temperature. When the mixture was completely dry, we found two types of crystalline solids, **1** and **2**, orange and yellow, respectively, which were easily separated.

Anal. Calcd for **1** $[Ce(NO_3)(Pic)(H_2O)_2(EO3)](Pic)$: C, 25.60; H, 2.63; N, 11.61. Found: C, 25.76; H, 2.10; N, 11.64%. m.p.: 446.9–452.9 K. IR (ν, cm^{-1}): 3376(st), 1579(s), 1567(s), 1380(st), 1342(st), 1083(s), 1062(s), 1274(s), 1488(s), 814(w), 933(s), 788(s).

Anal. Calcd for **2** $[Ce(NO_3)(Pic)(H_2O)_2(EO3)](Pic)$: C, 25.60; H, 2.63; N, 11.61. Found: C, 25.64; H, 2.33; N, 10.74%. m.p.: 370.3–384.3 K. IR (ν, cm^{-1}): 3450(b), 1571(s), 1537(s), 1384(s); 1347(s), 1085(s), 1071(s), 1288(s), 1484(s), 814(w), 938(s), 788(s).

2.3. *Physical measurement*

Carbon, hydrogen, and nitrogen analyses were made by a Perkin-Elmer 2400II elemental analyzer. IR spectra were recorded on a Perkin-Elmer system 2000 FTIR spectrophotometer from 4000 to 400 cm^{-1} by using KBr pellets for solid samples. For a liquid sample, a thin layer of sample was applied to the surface of a KRS-5 (Thallium bromoiodide).

PL measurements of the solid state were made at room temperature using a Jobin Yvon HR800UV system. A HeCd laser with wavelength at 325 nm was used for excitation light source.

2.4. *X-ray crystallographic study*

X-ray diffraction data of **1** and **2** were collected from single crystals by using a Bruker APEX2 area-detector diffractometer with graphite monochromatic Mo-Kα radiation and a detector distance of 5 cm. Data were analyzed with APEX2 software [8]. The collected data were reduced by using the SAINT program and empirical absorption corrections were applied using SADABS [8]. All structures were solved by direct methods and refined with full-matrix least-squares using SHELXTL [9]. All non-hydrogen atoms were refined anisotropically. Hydrogens were located from difference Fourier maps and were isotropically refined. The final refinement converged well. Data for publication were prepared with SHELXTL [9] and PLATON [10]. Two carbons (C1 and C2) in **1** are disordered over two positions with refined occupancies of 72 : 28 and 65 : 35. The thermal parameters of C1B and C2B atoms are higher than that found for C1A and C2A atoms. Thus, the C1B and C2B atoms are omitted for clarity in figure 1. Data collections and refinement parameters are summarized in table 1. Selected bond lengths, angles, and torsion angles are listed in table 2.

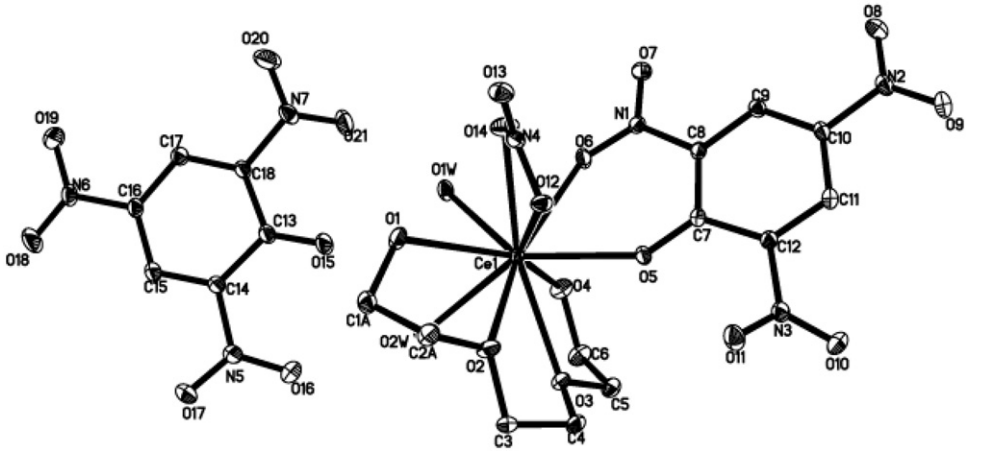

Figure 1. Molecular structure of **1** with 50% probability ellipsoids. The hydrogen atoms are omitted for clarity.

Table 1. Summary of crystallographic data and refinement for the cerium complexes.

Parameter	Compounds	
	1	**2**
Empirical formula	$C_{18}H_{22}N_7O_{23}Ce$	$C_{18}H_{22}N_7O_{23}Ce$
Formula weight	844.55	844.55
Temperature (K)	100	100
Volume (Å^3)	1433.21(3)	1416.74(3)
Crystal system	Triclinic	Triclinic
Space group	*P-1*	*P-1*
Unit cell dimensions (Å, °)		
a	7.1543(1)°	7.1099(1)°
b	8.3326(1)°	14.6948(2)°
c	24.5238(3)°	15.1659(2)°
α	95.290(1)	66.777(1)
β	91.214(1)	85.046(1)
γ	99.860(1)	76.646(1)
Z	2	2
Calculated density (g cm^{-3})	1.957	1.980
Absorption coefficient μ (mm^{-1})	1.703	1.723
F(000)	842	842
Crystal size (mm^3)	0.17 × 0.35 × 0.43	0.20 × 0.26 × 0.41
θ range for data collection (°)	0.83–32.50	1.46–37.50
Limiting indices	$-10 \le h \le 10$; $-12 \le k \le 12$; $-34 \le l \le 37$	$-12 \le h \le 12$; $-25 \le k \le 25$; $-25 \le l \le 25$
Reflections collected	41243	74365
Independent reflection	10334 [R(int) = 0.020]	14791 [R(int) = 0.026]
Refinement method	Full-matrix least-squares on F^2	Full-matrix least-squares on F^2
Data/restraint/parameter	10334/0/465	14791/0/437
Goodness-of-fit on F^2	1.228	1.084
Final R indices [$I > 2\sigma(I)$]	$R_1 = 0.019$, $wR_2 = 0.049$	$R_1 = 0.032$, $wR_2 = 0.086$
R indices (all data)	$R_1 = 0.020$, $wR_2 = 0.056$	$R_1 = 0.034$, $wR_2 = 0.092$
Largest difference peak and hole (e Å^{-3})	1.002 and −0.848	5.644 and −5.272

3. Results and discussion

3.1. *Physical properties and spectral analysis*

Two colors of single crystals of [Ce(NO$_3$)(Pic)(H$_2$O)$_2$(EO3)](Pic) have been synthesized by one-pot reaction of cerium nitrate, the EO3 ligand and HPic in a 1 : 4 : 3 (Ce : Pic : EO3) ratio. The cerium nitrate releases two NO_3^- while the third NO_3^- remains in the complexes, as competition between the NO_3^- and Pic anions. A small amount of water in the mixture helped the complexes form more readily due to the small chain length of the EO3 ligand [11].

The elemental analysis in general proves the suggested molecular formula of the cerium complexes. The complexes are stable to air and moisture and have m.p. in the range 446.9–452.9 and 370.3–384.3 K, respectively, for **1** and **2**. Both compounds are soluble in dimethyl sulfoxide, slightly soluble in methanol, water, and acetone, but completely insoluble in chloroform, ethyl acetate, or toluene.

The IR spectrum of free EO3 had a broad stretching band of ν(O–H), ν(C–C), and ν(C–O–C) at 3368, 1247, and 1115–1071 cm^{-1}, respectively [7]. Upon complexation, the bands were shifted toward the free EO3 and Pic ligands. Generally, ν(O–H) of free EO3 shifts to higher frequency by 8 and 82 cm^{-1} for **1** and **2**, respectively. The ν(C–O)

Table 2. Selected bond lengths (Å), angles (°) and torsion angles (°) for the cerium complexes.

	Length (Å)			Angle (°)			Torsion angle (°)	
Bond	**1**	**2**	Bond	**1**	**2**	Atom	**1**	**2**
Ce1–O1	2.585(1)	2.519(1)	O1–Ce1–O2	62.8(3)	61.9(4)	O1–C1–C2–O2	–	53.7(2)
Ce1–O2	2.590(1)	2.637(1)	O2–Ce1–O3	62.3(3)	60.8(4)	O1–C1A–C2A–O2	−56.2(3)	–
Ce1–O3	2.559(1)	2.661(1)	O3–Ce1–O4	62.8(3)	61.3(4)	O1–C1B–C2B–O2	57.3(6)	–
Ce1–O4	2.527(1)	2.540(2)	O4–Ce1–O1	141.7(4)	164.0(5)	O2–C3–C4–O3	55.4(1)	−55.3(2)
Ce1–O5	2.404(1)	2.380(1)	O12–Ce1–O14	48.3(3)	49.30(4)	O3–C5–C6–O4	55.2(2)	55.0(2)
Ce1–O6	2.617(1)	–	O2W–Ce1–O1W	70.27(3)	135.46(4)	Average O–C–C–O	56.0(3)	54.6(2)
Ce1–O12	2.637(1)	2.596(1)	O1–Ce1–O1W	75.64(4)	81.07(4)	C2–O2–C3–C4	–	−171.0(1)
Ce1–O14	2.632(1)	2.597(1)	O4–Ce1–O1W	77.29(4)	85.42(4)	C2A–O2–C3–C4	−169.8(2)	–
Ce1–O1W	2.467(1)	2.553(1)	O2W–Ce1–O1	70.16(4)	69.71(4)	C2B–O2–C3–C4	167.6(3)	–
Ce1–O2W	2.589(1)	2.489(1)	O2W–Ce1–O4	75.52(4)	115.77(4)	C3–O2–C2–C1	–	171.9(1)
Average C–O	1.453(4)	1.440(3)	O3–Ce1–O14	159.38(3)	77.75(4)	C3–O2–C2A–C1A	−113.7(2)	–
Average C–C	1.499(4)	1.499(2)	O5–Ce1–O12	73.04(3)	130.2(4)	C3–O2–C2B–C1B	−178.6(4)	–
			O5–Ce1–O14	91.73(4)	152.9(4)	C4–O3–C5–C6	167.9(1)	176.2(1)
			Average C–O–C	111.9(2)	110.9(1)	C5–O3–C4–C3	−167.0(1)	−178.0(1)
			Average O–C–C	106.7(2)	107.1(1)	Average C–O–C–C	160.8(2)	174.8(1)

shift to lower values by 32 and 30 cm^{-1} for **1** and **2**, respectively, indicating chelation of oxygen from EO3 by Ce(III). The strong ν(C–H) in EO3 at 2879 cm^{-1} appeared weak at 2959 cm^{-1} in compounds, indicating that EO3 rearranged to a pseudo-cyclic conformation [7, 12–15]. The disappearance of the phenolic out-of-plane bending vibration of free HPic at 1155 cm^{-1} in spectra of the complexes confirmed replacement of hydrogen by Ce(III) [7, 12–15]. Vibrational bands due to Pic anions ($\nu_{as}(NO_2)$ 1579–1537 cm^{-1} and $\nu_s(NO_2)$ 1384–1342 cm^{-1}) indicate that, at least in part, they are bidentate through the phenolic and *ortho*-nitro oxygens. The broad ν(O–H) occurred as expected at 3376 and 3450 cm^{-1} indicating that water molecules are present in the compounds, confirming the elemental analysis and decomposition.

Absorption bands assigned to the coordinated nitrate are observed at 1488–1483 cm^{-1} (ν1), 1024 cm^{-1} (ν2), 813 cm^{-1} (ν3), and 1327 cm^{-1} (ν4). From ν_a(N–O) and ν_s(N–O) of nitrate, the structures of both isomers could be elucidated. Separation of the two strongest frequency values [ν1–ν4] are 156 and 161 cm^{-1}, clearly establishing that the nitrate group coordinates bidentate to Ce(III) [16–18].

3.2. *X-ray studies*

Crystallographic data of the two isomers of $[Ce(NO_3)(Pic)(H_2O)_2(EO3)](Pic)$ were collected at the same temperature (100 K). Both have a triclinic crystal lattice, but different unit cell dimensions and volume. The Pic anions are capable of coordinating monodentate, bidentate, and tridentate [19]. The most favorable site is the negatively charged phenolic oxygen due to ion–ion interaction [20]. In addition, the oxygen of *ortho*-nitro group is also favorable due to charge localization on this oxygen. The phenolic and *ortho*-nitro oxygens had the short distance, 2.675 Å, an effective bidentate mode with both charge and dipole binding ability. The conformation and atom connectivity in two isomers were not similar. In **1** the Pic is bound bidentate through oxygen from phenol and *ortho*-nitro oxygen, while in **2** the Pic is bound monodentate through oxygen from the phenol.

Ce(III) has different coordination number and coordination structures in **1** and **2**. The asymmetric unit of the two complexes contain two crystallographically independent $[Ce(NO_3)(Pic)(H_2O)_2(EO3)]^+$ and Pic counteranion. Ce(III) in **1** is coordinated to 10 oxygens from Pic, EO3, one nitrate, and two waters in a distorted bicapped square antiprismatic geometry. The geometry was slightly distorted due to a bond angle nearly 180° for O3 and O14 at the top in the capping position, 159.38(3)° (figure 2). The Pic counteranion was situated toward $[Ce(NO_3)(Pic)(H_2O)_2(EO3)]^+$ with angle between two planes of Pic being 16.31(7)° (figure 1). The positions of Pic counteranion is similar to those of coordinated Pic in $[La(Pic)_2(EO3)_2](Pic)$ and $[Ln(Pic)_2(EO5)](Pic)$ [7, 12–14], and $[Gd(H_2O)(Pic)_2(EO4)](Pic) \cdot 0.5CH_3OH$ [21]. The coordination number in $[Ce(NO_3)(Pic)(H_2O)_2(EO3)](Pic)$ is comparable with those of Eu(III), Tb(III), and Gd(III) dinuclear complexes [22, 23]. This finding extends the structures of lanthanide complexes with high coordination numbers and show the efficiency of structurally flexible EO3 and electron-rich Pic in chelation.

In **2** the Pic counteranion is located at lower position to $[Ce(NO_3)(Pic)(H_2O)_2(EO3)]^+$ with angle between two planes of Pic anions being 1.69(8)° (figure 3). Effective delocalization of the negative charge among the widely separated *ortho* and *para*-nitro oxygens explained that the existence and stability of complexes in which the Pic

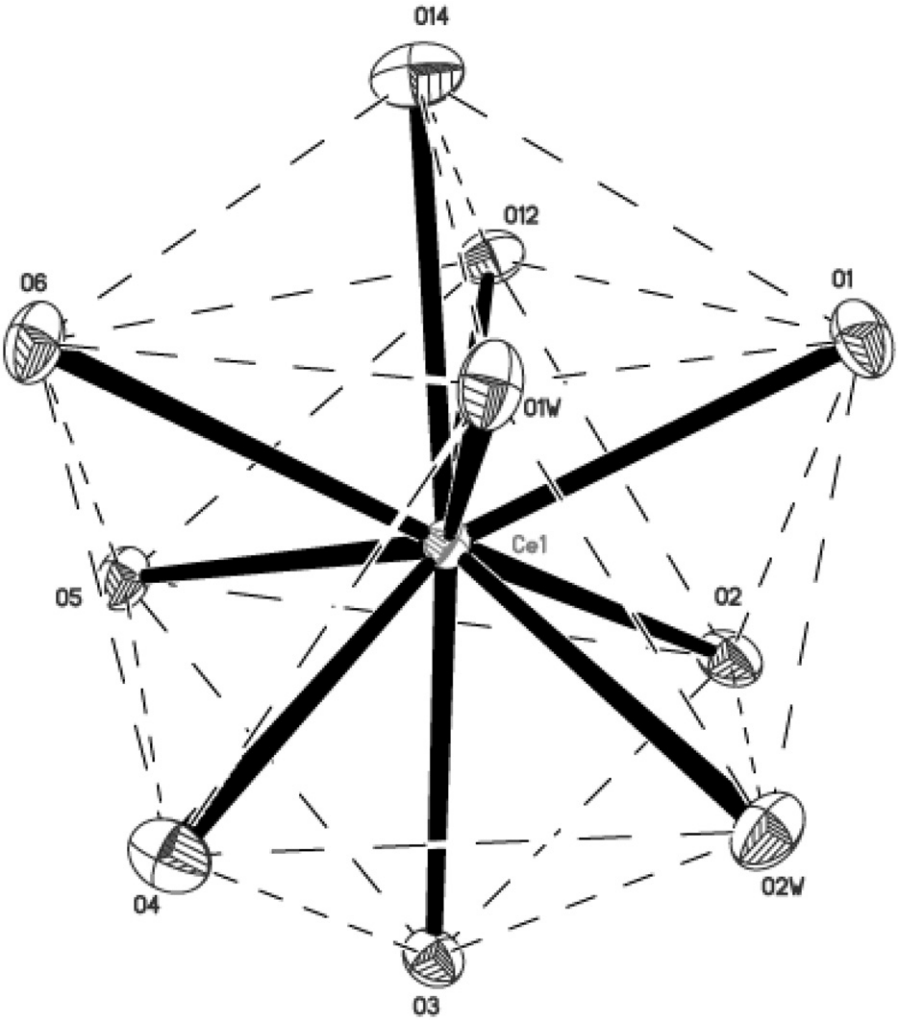

Figure 2. Coordination geometry around Ce1 in **1** as a distorted bicapped square antiprismatic with the O3 and O14 at the top in the capping position.

counteranion is excluded from the inner-coordination sphere. As in **1**, **2** has the same number of waters, nitrate, EO3, and Pic, forming a nine-coordinate in a distorted tricapped trigonal geometry (figure 4). O2, O5, and O12 are capping position with point symmetry C_1. The Ce1 lies on the trigonal plane from O2–O5–O12 with maximum deviation of −0.001(1) Å for Ce1. The Ce1 is at the base of the triangle of O2–O12–O5 with a maximum deviation of 0.010(1) Å for Ce1. Figure 4 shows the edge lengths between O3–O1W [3.217 Å] and O14–O1 [3.327 Å] are not coplanar. In addition, the O3–O14 [3.300 Å], O14–O12 [2.166 Å], O1–O5 [3.249 Å], O1–O2 [2.655 Å], and O3–O4 [2.654 Å] edge lengths are neither coplanar nor parallel.

In $[Ce(NO_3)(Pic)(H_2O)_2(EO3)](Pic)$, coordinated waters were positioned between O1 and O4 of the terminal alcohol groups with bond angles of 70.27(3)° and 135.46(4)° for **1** and **2**, respectively. **1** and **2** crystallize following a lengthy (7 months) evaporation,

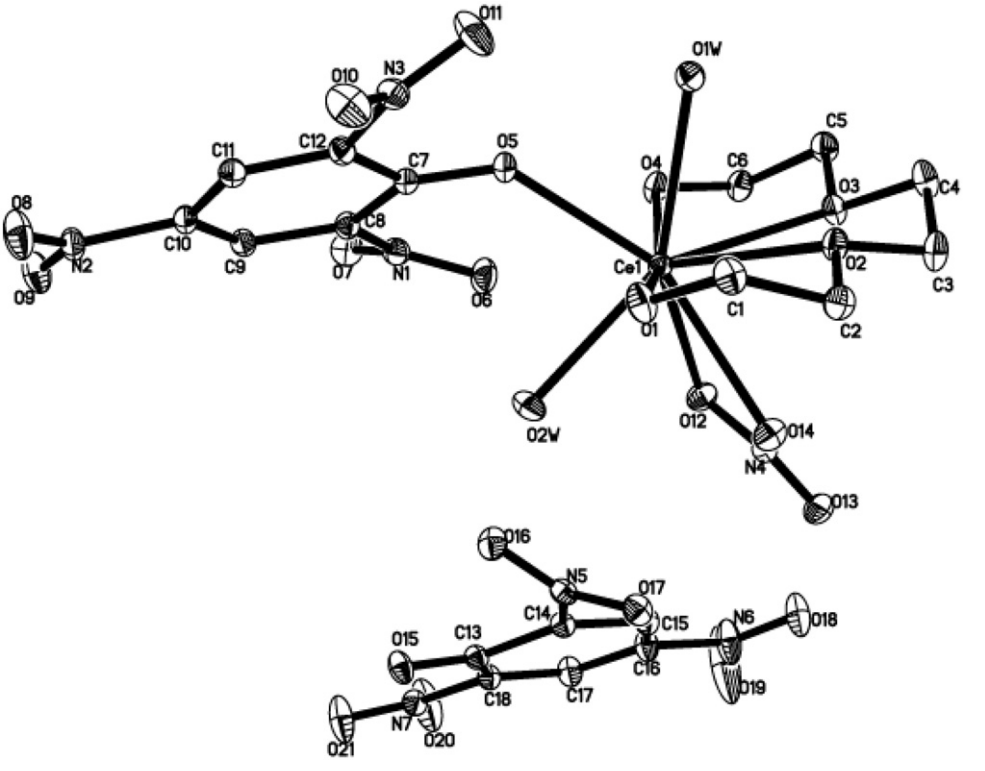

Figure 3. Molecular structure of **2** with 50% probability ellipsoids. The hydrogen atoms are omitted for clarity.

suggesting that both isomers are more thermodynamically stable and efficient in crystal packing than those found in $[La(Pic)_2(EO3)_2](Pic)$ [7]. Calculated densities of **1** and **2** are similar, 1.957 and 1.980 g cm^{-3}, respectively.

In **1**, the coordinated Pic O5/C7/C8/N1//O6 and nitrato O12/N4/O14/O13 fragments were situated on the same sides of the coordination sphere and are also planar, with maximum deviation being −0.139(1) Å for O5 in the picrato fragment (figure 1). However, the Ce1 is slightly deviated by −0.645(1) and 0.602(1) Å from both fragments. Both fragments are inclined to each other by 77.93(7)° in **1**. The O5–Ce1–O12 and O5–Ce1–O14 have bond angles of 73.04(3)° and 91.73(4)°, respectively; torsion angles of O12–Ce1–O5–C7 and O14–Ce1–O5–C7 are −85.92(15)° and −40.81(16)°.

In **2**, the nitrato fragment is almost linear with the picrato fragment (figure 3). The coordinated Pic O5/C7/C8/N1//O6 and nitrato O12/N4/O14/O13 fragments were situated on different sides of the coordination sphere and also are planar, with maximum deviation of 0.491(1) Å for O6 in the picrato fragment. However, the Ce1 deviates by 1.492(1) and 0.572(1) Å from both fragments. Both fragments are inclined to each other by 56.11(9)°. The O5–Ce1–N4, O5–Ce1–O12, and O5–Ce1–O14 have bond angles of 150.0(4), 130.2(4), and 152.9(4)°, respectively; torsion angles of N4–Ce1–O5–C7, O12–Ce1–O5–C7, and O14–Ce1–O5–C7 are 30.9(2), 54.6(2) and −22.5(2)°.

As expected, the Ce−$O_{alcohol}$ bond lengths are shorter than the Ce−O_{ether} bond lengths (table 2). The average Ce–$O_{alcohol}$ and Ce–O_{ether} bond lengths are 2.556(1),

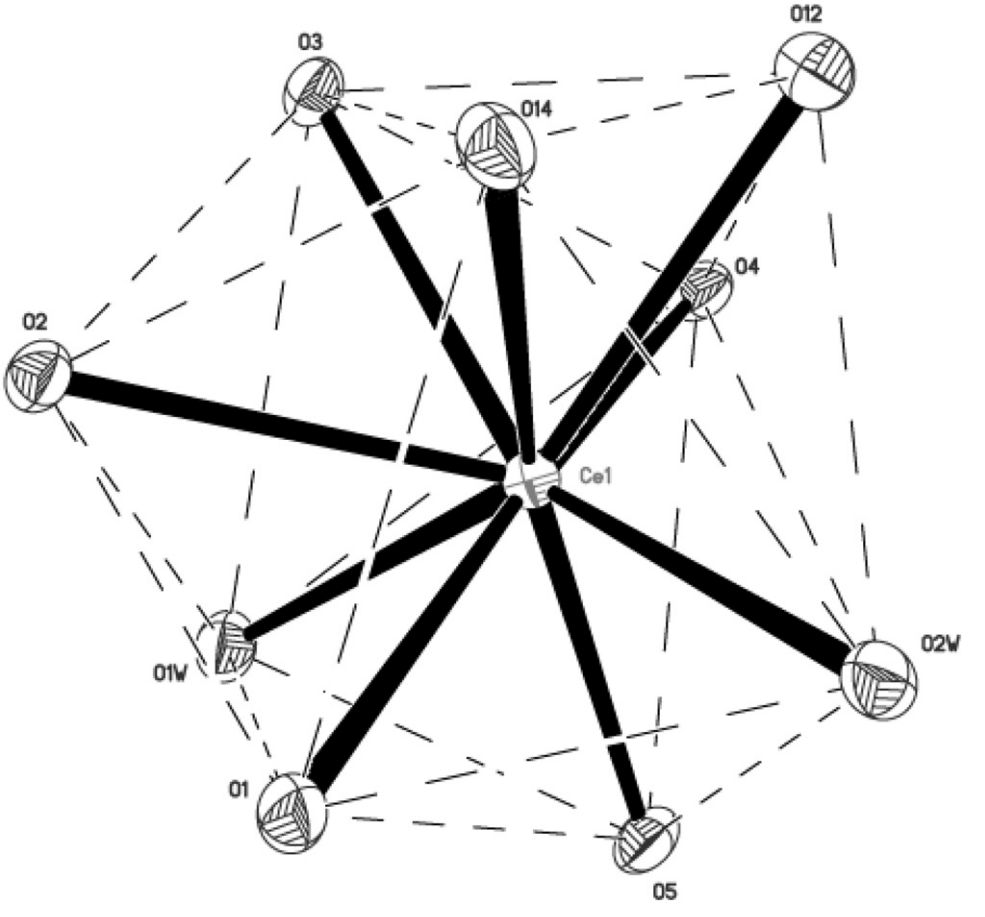

Figure 4. Perspective view around Ce1 in **2** as a distorted tricapped trigonal prismatic with the O2, O5, and O12 in the capping position.

2.529(1) Å and 2.575(1), 2.649(1) Å for **1** and **2**, respectively. The average Ce−O_{EO3} bond lengths are shorter than those found in the $[CeCl(OH_2)(EO3)_2]Cl_2$ [2.650(2) Å] [5] and $[Ce(NO_3)_3(OH_2)(EO3)] \cdot CH_3CN$ [2.630(2) Å] complexes [6]. The average Ce−O_{phenol} bond lengths are the shortest, i.e., 2.404(10) and 2.380(1) Å for **1** and **2**, respectively. The shortness of these bonds is caused by higher electron density on the phenolic oxygen of Pic [7, 12–14, 24, 25] and smaller steric effect [26]. In **2**, O6 from *ortho*-nitro group of the coordinated Pic anion did not participate in coordination with length of 3.076 Å. The Ce−O_{nitro} bond was the longest [2.617(1) Å], reflecting the lower electron density of the *ortho*-nitro oxygen than the phenolic oxygen of Pic. The same trend was observed in $[La(Pic)_2(EO3)_2](Pic)$ of 2.741(4) Å [7], $[Pr(Pic)_2(EO5)](Pic)$ of 2.582(4) Å [12], $[Sm(Pic)_2(EO5)](Pic)$ of 2.519(3) Å [14], and $[Eu(Pic)_2(EO5)](Pic)$ of 2.496(2) Å [13].

In the acyclic EO3 ligand, the bond lengths of C−C and C−O and the bond angles in C−O−C and O−C−C were unchanged and comparable to the values seen in the other Ln–EO3 complexes [7]. The O−Ce−O bond angle between adjacent oxygens

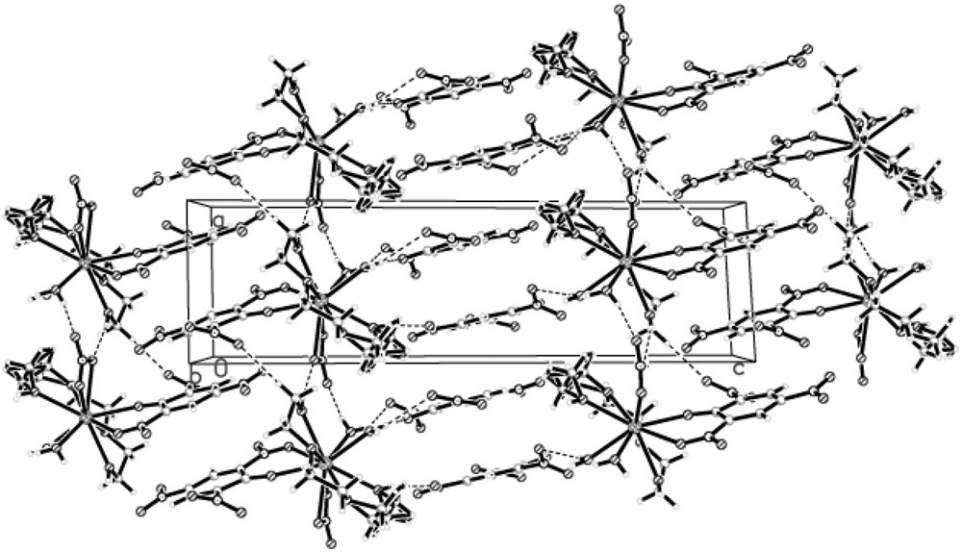

Figure 5. The crystal packing of **1** showing a 1-D network viewed down the *b*-axis. The hydrogen bonds are indicated by dashed lines.

in the inner coordination sphere of the complexes was approximately the same, slightly larger than 60°. However, the O1−Ce1−O4 bond angle in the terminal alcohol group in **2** is larger than 22° found in **1** (table 2). The O1−Ce1−O4 bond angle in **1** was quite close to the O1−La1−O4 bond angle in $[La(Pic)_2(EO3)_2](Pic)$ [7]. The chain length of the acyclic PEG ligand also influenced the bond angle between the adjacent oxygen terminal alcohol in the inner coordination, e.g., the $[Ln(Pic)_2(EO5)](Pic)$ complexes of 66.4(1)°–72.0(6)° [7, 12–14] were narrower than those found in cerium complexes. The acyclic EO3 displayed a series of *anti* and *gauche* torsion angles for C−O and C−C bonds. In **1** and **2**, the average O−C−C−O torsion angle was 56.0(3)° and 54.6(2)° and the EO3 showed a geometric conformational pattern of g^- or $g^+ g^+ g^+$ and $g^+ g^- g^+$, respectively. All the C−O−C−C torsion angles are *anti*.

The aromatic part of the coordinated Pic was planar with maximum deviation of −0.042(1) Å for C7 and −0.031(1) Å for C12 in **1** and **2**, respectively. One peculiarity of the coordinated Pic is the shortening of the $C-O_{phenol}$ bonds relative to bonds in the acid, 1.323(3) Å [27]. The $C-O_{phenol}$ bond lengths of the coordinated Pic in **2** [1.274(18) Å] is longer than found in **1** [1.263(2) Å] because of monodentate or bidentate Pic modes. The $C-O_{phenol}$ of Pic is a counteranion and shorter than that found in coordinated Pic, i.e., 1.251(2) and 1.255(2) Å, respectively, for **1** and **2**.

Both terminal alcohols of EO3 can act as anchoring points with locally fixed donor centers to which Ce(III) can bind with a certain number of donor sites remaining a prerequisite for complex formation. There are different types of hydrogen bonding and π–π interactions in both isomers that give rise to different supramolecular architectures (figures 5 and 6). Through hydrogen bonding and π–π stacking interactions, **1** and **2** form 1-D supramolecular sheet structures extending in the [100] plane. In **1**, the sheets are oriented in the same direction and alternate with respect to coordinated Pic and Pic counteranion (figure 5). In **2**, the sheets are oriented in different

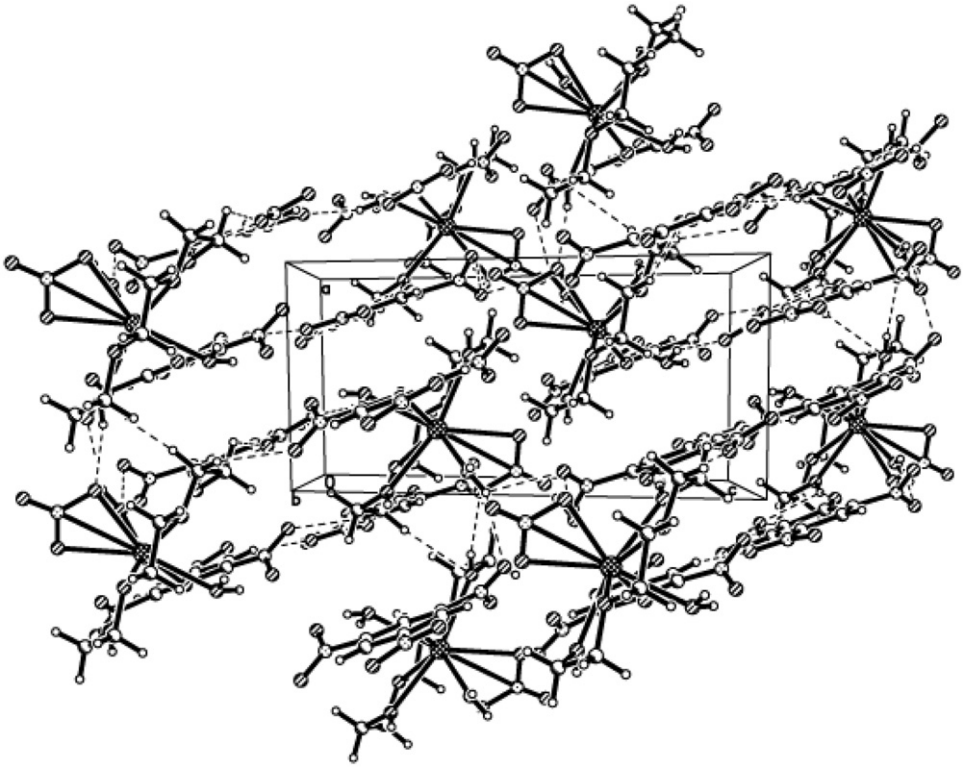

Figure 6. The crystal packing of **2** showing a 1-D network viewed down the *b*-axis. The hydrogen bonds are indicated by dashed lines.

directions (figure 6). Adjacent molecules from different asymmetric units are linked by intra and intermolecular O–H···O and C–H···O hydrogen bonds along the *a*-axis (tables 3a and b). In **1**, the terminal alcohols formed intermolecular O–H···O hydrogen bonds with acceptor oxygens of nitro. Two intramolecular bifurcated hydrogen bonds O1W–H11W···O15, O1W–H11W···O21, O2W–H22W···O15, and O2W–H22W···O16 were observed in **1** (table 3a). In **2**, two weak intramolecular and two bifurcated hydrogen bonds of O1W–H11W···O11, O2W–H22W···O16, O1–H1C···O15, O1–H1C···O21, O2W–H22W···O7, and O2W–H22W···O16 were observed (table 3b).

The crystal structures are stabilized by π–π stacking. In **1**, the shortest π–π interaction involved the aromatic part of the Pic counteranion with face-to-face mode at 4.003(8) Å (symmetry $1-x, 1-y, 1-z$) with an angle between π–π and normal to plane of aromatic ring (C13–C18) of 29.74° (figure 5); π–π interactions from the aromatic part of Pic counteranion are not observed in **2**. However, the intermolecular π–π interaction between the alternating aromatic part of the coordinated Pic anion and the Pic counteranion with the centroid to centroid distance of 4.209(9) Å (symmetry $1-x, -y, 1-z$) with dihedral angle between planes (C7–C12) and (C13–C18) of 1.69° was observed in **2** (figure 6). One C11–H11A···Cg2 [3.260 Å] van der Waals interaction with symmetry code $2-x, -y, 1-z$ was observed in **2**.

Table 3. Geometrical parameters of intra- and intermolecular hydrogen bonding involved in **1** and **2**.

D–H···A	D–H (Å)	H···A (Å)	D···A (Å)	D–H···A (°)
(a) **1**				
O1–H1C···O19^{i}	0.80(3)	2.04(3)	2.805(2)	159(3)
O4–H4C···O12^{iii}	0.75(3)	2.06(3)	2.779(2)	163(2)
O1W–H11W···O15^{a}	0.82(3)	1.86(3)	2.658(2)	165(3)
O1W–H11W···O21^{a}	0.82(3)	2.49(3)	2.942(2)	116(2)
O2W–H12W···O20^{ii}	0.75(3)	2.34(3)	3.042(2)	157(3)
O1W–H21W···O13^{iii}	0.83(3)	1.93(3)	2.757(2)	170(3)
O2W–H22W···O15^{a}	0.83(3)	2.01(3)	2.773(2)	153(3)
O2W–H22W···O16^{a}	0.83(3)	2.46(3)	3.075(2)	132(2)
C3–H3B···O14^{ii}	0.970	2.526	3.170(2)	123.8
C4–H4A···O11^{a}	0.969	2.520	3.457(2)	162.5
C4–H4B···O6^{ii}	0.970	2.550	3.433(2)	151.5
C5–H5A···O13^{iv}	0.970	2.414	3.222(2)	140.4
C5–H5B···O5^{a}	0.969	2.569	3.121(2)	116.3
C6–H6A···O11^{iii}	0.970	2.405	3.374(2)	177.5
(b) **2**				
O1–H1C···O15^{i}	0.930	1.752	2.652(2)	162.2
O1–H1C···O21^{i}	0.930	2.449	2.957(2)	114.5
O4–H4C···O14^{ii}	0.821	2.079	2.850(2)	156.2
O1W–H11W···O11^{a}	0.850	2.357	3.129(2)	151.4
O2W–H12W···O16^{i}	0.849	2.367	3.003(2)	132.1
O1W–H21W···O20^{iii}	0.851	2.120	2.907(2)	153.7
O2W–H22W···O7^{iv}	0.851	2.316	3.047(2)	144.3
O2W–H22W···O16^{a}	0.851	2.515	2.902(2)	108.7
C1–H1A···O21^{i}	0.970	2.476	2.924(2)	107.9
C2–H2A···O10^{v}	0.970	2.459	3.323(2)	148.2
C2–H2B···O4^{iii}	0.970	2.575	3.527(2)	166.9
C3–H3B···O18^{vi}	0.970	2.481	3.375(3)	153.1
C4–H4B···O9^{vii}	0.970	2.552	3.481(3)	160.4
C11–H11A···O19^{viii}	0.931	2.338	3.240(3)	163.1

D = donor and A = acceptor.
Symmetry codes for **1**: (i) $1-x, 1-y, 1-z$; (ii) $x, 1+y, z$; (iii) $1+x, y, z$; (iv) $1-x, 2-y, 1-z$.
Symmetry codes for **2**: (i) $2-x, -y, 1-z$; (ii) $x, y, 1+z$; (iii) $1+x, y, z$; (iv) $-1+x, y, z$; (v) $2-x, -y, 2-z$; (vi) $2-x, -y, 1-z$; (vii) $x, 1+y, z$; (viii) $x, -1+y, 1+z$.
[a]Intramolecular hydrogen bonding.

4. PL studies

Emission spectra of the free EO3 ligand and its complexes in the solid state were evaluated at room temperature based on D2 filter measurement. Free EO3 exhibits intense broad emission bands at 406 and 485 nm ($\lambda_{exc.} = 325$ nm) and HPic has a broad band with center at 537 nm [28]. Isomers **1** and **2** are emissive at room temperature and show an intraligand fluorescence emission comparable to free EO3 with maximum at 540 nm. The red-shift emission is from intraligand fluorescent emission [28, 29]. The emission intensity in the strong peak for **1** (43×10^4 a.u.) is higher than that found in **2** (15×10^4 a.u.). The structure of **1** may be more favorable for intramolecular energy transfer as shown by shorter Ce–O_{EO3} bond lengths between EO3 and Ce(III). In addition, the coordination number in **1** is higher than **2**. A broad peak at 515–540 nm (19417–18518 cm^{-1}) is a typical emission property of Ce(III) from the electric dipole originating from the $5d \rightarrow 4f$ transition [30].

The main luminescence bands of [Ce(NO_3)(Pic)(H_2O)$_2$(EO3)](Pic) appear in the same region as Tb(III)–Tb(III) and Tb(III)–Gd(III) dinuclear complexes [22, 23]. The electronic structure of those La(III) ions could be similar, while the efficiency of intramolecular energy transfer from ligand to La(III) in those different complex determined by the structures result in different emission efficiency.

5. Conclusions

[Ce(NO3)(Pic)(H_2O)$_2$(EO3)](Pic) with two different isomers has been synthesized and structurally characterized. Both isomers have different crystal colors, and the Ce(III) ion has different coordination structures. The PL intensity is affected by coordination number. The complexes display a red-shift emission peak in the solid state compared with the free acyclic EO3 ligand.

Supplementary material

CCDC 684230 and CCDC 684231 supplementary crystallographic data for **1** and **2**, respectively, can be obtained free of charge from the Cambridge Crystallographic Data Center via www.ccdc.cam.ac.uk/data_request/cif.

Acknowledgments

We thank Universiti Sains Malaysia and the Malaysian Government for supporting this research with grants FRGS and SAGA. The authors thank Dr Anwar Usman for text revision and helpful suggestions.

References

[1] R.D. Rogers, J. Zhang, C.B. Bauer. *J. Alloys Compounds*, **249**, 41 (1997).
[2] Y.-J. Zhu, J.-X. Chen, W.-H. Zhang, Z.-G. Ren, Y. Zhang, J.-P. Lang, S.-W. Ng. *J. Organomet. Chem.*, **690**, 3479 (2005).
[3] J.-G. Bünzli, N. André, M. Elhabiri, G. Muller, C. Piguet. *J. Alloys Compounds*, **303–304**, 66 (2000).
[4] Y. Hirashima, T. Tsutsui, J. Shiokawa. *Chem. Lett.*, 1405 (1982).
[5] R.D. Rogers, R.D. Etzenhouser, J.S. Murdoch. *Inorg. Chim. Acta*, **196**, 73 (1992).
[6] R.D. Rogers, C.B. Bauer. In *Comprehensive Supramolecular Chemistry*, J.L. Atwood (Ed.), Vol. 1, Chap. 8, p. 321, Pergamon Express, Illinois, USA (1996).
[7] M.I. Saleh, E. Kusrini, H.-K. Fun, B.M. Yamin. *J. Alloys Compounds*, **474**, 428 (2009).
[8] Bruker, APEX2, SAINT and SADABS. Bruker AXS Inc., Madison, WI, USA (2005).
[9] G.M. Sheldrick. *Acta Crystallogr., Sect. A*, **64**, 112 (2008).
[10] A.L. Spek. *J. Appl. Crystallogr.*, **36**, 7 (2003).
[11] Y. Hirashima, T. Tsutsui, J. Shiokawa. *Chem. Lett.*, 1405 (1982).
[12] M.I. Saleh, E. Kusrini, R. Adnan, I.A. Rahman, B. Saad, A. Usman, H.-K. Fun, B.M. Yamin. *J. Chem. Crystallogr.*, **35**, 469 (2005).
[13] M.I. Saleh, E. Kusrini, B. Saad, R. Adnan, A. Salhin, B.M. Yamin. *J. Lumin.*, **126**, 871 (2007).

[14] M.I. Saleh, E. Kusrini, R. Adnan, B. Saad, H.-K. Fun, B.M. Yamin. *J. Mol. Struct.*, **837**, 169 (2007).
[15] F. Vögtle, E. Weber. *Angew. Chem. Int. Ed. Engl.*, **18**, 753 (1979).
[16] Y.-L. Guo, W. Dou, Y.-W. Wang, W.-S. Liu, D.-Q. Wang. *Polyhedron*, **26**, 1699 (2007).
[17] W. Carnall, S. Siegel, J. Ferrano, B. Tani, E. Gebert. *Inorg. Chem.*, **12**, 560 (1973).
[18] K. Nakamoto. *Infrared and Raman Spectra of Inorganic and Coordination Compounds*, 3rd Edn, John Wiley, New York (1978).
[19] U. Oisher, F. Feinberg, F. Frolow, G. Shohum. *Pure Appl. Chem.*, **68**, 1195 (1996).
[20] U. Olsher, R.M. Izatt, J.B. Bradshaw, N.K. Dalley. *Chem. Rev.*, **91**, 137 (1991).
[21] E. Kusrini, M.I. Saleh, R. Kia, H.K. Fun. *Acta Crystallogr., Sect. E*, **64**, m1179 (2008).
[22] Y. Zhang, X. Li, Y. Li. *J. Coord. Chem.*, **62**, 583 (2009).
[23] Y.-P. Liu, D.-F. Rong, H.-T. Xia, D.-Q. Wang, L. Chen. *J. Coord. Chem.*, **62**, 1835 (2009).
[24] M.I. Saleh, E. Kusrini, H.-K. Fun, B.M. Yamin. *J. Organomet. Chem.*, **693**, 2561 (2008).
[25] L. Fan, W. Liu, X. Gan, N. Tang, M. Tan, W. Jiang, K. Yu. *Polyhedron*, **19**, 781 (2000).
[26] Y.-L. Zhang, W.-H. Jiang, W.-S. Liu, Y.-H. Wen, K.-B. Yu. *Polyhedron*, **22**, 1695 (2003).
[27] M.I. Saleh, E. Kusrini, M.R. Mustaqim, H.-K. Fun. *Acta Crystallogr., Sect. E*, **64**, o1318 (2008).
[28] E. Kusrini, M. Idiris Saleh, C. Lecomte. *Spectrochim. Chim. Acta, Part A*, **74**, 120 (2009).
[29] L.-Q. Yu, R.-D. Huang, Y.-Q. Xu, T.F. Liu, W. Chu, C.W. Hu. *Inorg. Chim. Acta*, **361**, 2115 (2008).
[30] M.F. Reid, V.L. Pieterson, R.T. Wegh, A. Meijerink. *Phys. Rev. B: Condens. Matter*, **62**, 14744 (2000).